Journal of Sustainable Development of Energy, Water and Environment Systems

http://www.sdewes.org/jsdewes

Year 2026, Volume 14, Issue 2, 1400668

Original Research Article

Experimental Study of Pulsating Heat Pipe to Improve Photovoltaic Efficiency

***Yuli Setyo Indartono*[*1], *Abdul Aziz Khalilurrahman*[1], *Ivan Farozan*[1]**

[1]Faculty of Mechanical and Aerospace Engineering, Institut Teknologi Bandung, Ganesha 10, Bandung 40132, Indonesia

e-mail: ysindartono@itb.ac.id

Cite as: Setyo Indartono Y, Aziz Khalilurrahman A, Farozan I, Predicting Experimental Study of Pulsating Heat Pipe to Improve Photovoltaic Efficiency. J.sustain. dev. energy water environ. syst., 14(2), 1400668, 2026,
DOI: https://doi.org/10.13044/j.sdewes.d13.0668

ABSTRACT

Pulsating Heat Pipe offers an effective passive cooling method to mitigate the efficiency drop in solar photovoltaics caused by excessive temperature. In the present work, single-loop Pulsating Heat Pipe using methanol and ethanol working fluids with filling ratios of 35%, 45%, and 55% with initial pressures of 30 kPa, 50 kPa, and 100 kPa were tested at power input of 13.8-60 W. The factors that affect startup performance and thermal resistance were studied experimentally on a lab scale. The results demonstrated that Pulsating Heat Pipe charged with methanol shows superior startup performance and lower thermal resistance compared to ethanol. Experimental results indicate that a 35% filling ratio provides the fastest startup condition, while the best thermal performance is obtained at 45%. Decreasing the initial pressure on Pulsating Heat Pipe can accelerate startup and improve thermal performance. Integrating Pulsating Heat Pipe with the solar panel can potentially reduce the panel temperature by up to 5.1 °C.

KEYWORDS

pulsating heat pipe, photovoltaic cooling, solar energy, passive cooling, filling ratio, initial pressure, startup performance, thermal resistance.

INTRODUCTION

In 2022, 80% of global energy needs will be supplied by fossil fuels [1]. A study conducted by Le quere et al. [2] stated that fossil fuel consumption, especially from the combustion of fossil fuels such as coal, oil, and natural gas, is the main cause of greenhouse gas emissions that accelerate global warming, and its dependence raises concerns about the distribution, supply, and price volatility. Renewable energy is an alternative in efforts to reduce carbon emissions by producing clean energy [3]. One of the renewable energies that is easily accessible and abundant is solar energy [4].

The increasing global interest in renewable energy has spurred significant developments in photovoltaic (PV) technology, positioning solar power as one of the most promising and sustainable electricity sources. However, the performance of PV modules is closely related to their operating temperature. When these modules heat up beyond the standard test condition (STC) of 25 °C, their electrical efficiency typically drops by about 0.5–0.7% for every degree Celsius increase [5]. This loss in efficiency due to heat is especially problematic in areas with intense solar radiation and high ambient temperatures. To counteract this, passive cooling methods, which do not require extra energy, have been identified as an effective way to

* Corresponding author

improve the efficiency and lifespan of PV modules [6]. Sutanto et al. [7] examined the use of passive cooling systems to increase savings of power and reduce operational costs.

The Pulsating heat pipe (PHP) is an example of a passive cooling method. PHP, also known as oscillating heat pipe (OHP), has garnered significant attention in recent years as a highly efficient and adaptable thermal management technology [8]. Unlike general heat pipes, a Pulsating Heat Pipe consists of a single capillary tube that contains multiple alternating evaporator and condenser sections [9]. It also has low thermal resistance, reliable operation, and high thermal conductivity [10]. A more uniform temperature distribution achieved through PHP cooling leads to an enhancement in system performance [11]. The operational principle of the PHP relies on the oscillatory flow of liquid-vapor slugs to transport thermal energy [12].

These wickless, passive heat transfer devices leverage the principles of two-phase flow and phase change to enable the efficient transport of heat over considerable distances, making them well-suited for addressing the ever-increasing thermal management challenges faced by modern microelectronic devices [13]. The fundamental operating principle of a PHP involves the cyclic evaporation and condensation of a working fluid within a meandering, capillary-sized tube [14]. As heat is applied to the evaporator section, the working fluid vaporizes, creating pressure differentials that drive the oscillatory motion of the liquid-vapor plugs [15]. Pressure disturbances are initiated by a temperature gradient across the tube's ends, where localized differences in heat transfer occur between the evaporator (heat-receiving) and condenser (heat-dissipating) sections, separated by an adiabatic zone [16]. This facilitates the transfer of heat from the evaporator to the condenser.

A study on the effectiveness of using PHP cooling systems to enhance the efficiency of solar photovoltaic panels in Malaysia was performed by Roslan and Hassim [12]. They attached a multi-turn closed-loop PHP made from a copper tube on the back surface of a PV module. The condenser section was put inside a still water box made from acrylic. They found up to 10.5 °C reduction in PV panel temperature, which leads to an 8.03% increase in energy production when incorporating a PHP on solar PV panels. Alizadeh et al. [17] conducted a numerical simulation study on the cooling of PV panels using a single-turn PHP to enhance their electrical efficiency. The simulated PHP used distilled water with a 40% filling ratio as the working fluid. The result was a 16.1 °C decrease in PV panel temperature and an 18% increase in electrical power output for 1000 W/m^2 solar irradiation. Two scenarios of utilizing a flat plate PHP as a cooling system for a PV panel were numerically studied by Alizadeh et al. [3]. The first scenario was a passive cooling system where natural convection cooled the condenser. In contrast, the second scenario was an active cooling system where the PHP's condenser was cooled by flowing water. Their study showed a lower PV temperature reduction by 14.6 °C and 22.2 °C at 1235 W/m^2 for the first and second scenarios, respectively.

A PHP system's performance is influenced by its geometries, operating conditions, and working fluid properties [18]. Extensive research has been conducted to elucidate the complex thermo-fluid dynamics underlying the operation of pulsating heat pipes, with a focus on optimizing their thermal performance [19]. The key geometrical parameters include the tube diameter and the number of turns [20]. The evaporator-to-condenser length ratio is a critical design parameter that governs the heat flux absorption capability of the pulsating heat pipe system [21]. The tube diameter is especially critical because it governs the formation of liquid slugs and vapor plugs by balancing surface tension against buoyancy forces [22]. Although smaller diameters improve performance by ensuring better vapor and liquid distribution, increased frictional losses can offset these benefits if the diameter becomes too small [23].

Furthermore, the number of turns in the evaporator section is crucial. The lowest number of cycles, eight cycles, reaches the dry point more quickly than those with more cycles [24]. Increasing turns enhances the stability condition within the PHP, ultimately improving performance [25]. In addition, using more than 16 turns, as Charoensawan et al. [26] suggested, generally ensures reliable performance across different orientations. The heat transfer process is further affected by the effective lengths of the evaporator, adiabatic, and condenser sections [21].

The optimal values of the length ratio between evaporator and condenser were determined by Liu et al. [27] on the thermal performance of aluminum-based heat exchangers based on their shape.

Operating conditions significantly impact performance, including PHP orientation, heat input, and filling ratio. The PHP's orientation, defined by the angle between the gravitational force and the channels, plays a critical role—even when the Bond number is small. In a vertical configuration, where the evaporator is positioned at the bottom and the condenser at the top, gravity returns liquid from the condenser to the evaporator, resulting in optimal "gravity-assisted" performance [13]. Conversely, in an "anti-gravity" configuration, where the evaporator and condenser are reversed, gravitational forces can hinder performance and may cause the evaporator to dry out at low heat inputs. In a horizontal orientation, where the channels are perpendicular to gravity, performance is less influenced by gravitational forces and, with a sufficient number of evaporator turns, can closely match that of the gravity-assisted setup [28]. The initial pressure of a PHP system also significantly affects its performance. A PHP with lower initial pressure had a lower evaporation section temperature [29].

Choosing the working fluid as the medium for heat transfer to reduce temperature is also a critical factor in designing a PHP system for cooling PV [8]. According to Ma [20], the selection is crucial due to the effects of fluid properties such as surface tension, thermal conductivity, latent heat, specific heat, boiling temperature, and viscosity. Working fluid with higher latent heat will transfer more energy per cycle when vaporizing, which can be beneficial at higher operating temperatures and heat loads [30]. Fluids with lower boiling points can start vaporizing at lower temperatures, which may result in more vigorous oscillatory motion at low heat fluxes or low-temperature applications [31]. In the bubble nucleation process, the latent heat of vaporization plays a critical role by determining the necessary surface superheat temperature for the inception and growth of a hemispherical vapor bubble [32]. In addition, fluid with lower viscosity may reduce frictional losses. Based on experiments conducted by Sutanto et al. [33], the operational temperatures of ground-mounted photovoltaic (PV) systems in Bandung City, Indonesia, were found to range between 35.9 ℃ and 62,1 ℃, with an average temperature of around 51.5 ℃. The average temperature observed by Sutanto et al. [33] indicates the need for a working fluid with a lower boiling temperature for a PHP system to cool a PV.

Qu et al. [29] investigated the influence of initial pressure in water-filled PHP and observed a reduction in thermal resistance with optimal pressure. Another research studied the effect of filling ratio by Clement and Wang [34] using R-123, acetone, and methanol at a pressure atmosphere, which found an optimal filling ratio range of 35%-55%.

Based on the works mentioned above, it can be concluded that PHP is a very complex system involving multiple aspects. Previous research has demonstrated the potential of PHPs for passive cooling of photovoltaic (PV) modules. However, the influence of initial pressure on the performance of methanol-based and ethanol-based PHP systems has not been comprehensively investigated at different initial pressures. The present study addresses this research gap by experimentally evaluating the thermal performance of PHPs using two different working fluids (methanol and ethanol) under varied initial pressures (30, 50, and 100 kPa), filling ratios (35%, 45%, and 55%), and heating powers (13.8–60 W).

Distinct from previous works, the condenser section in this study was cooled solely by natural convection, representing a realistic passive-cooling condition for PV modules. The temperatures of the evaporator, adiabatic, and condenser sections were measured to determine the thermal resistance for each configuration. Furthermore, the startup characteristics of the PHPs were analyzed and compared. In addition, another novelty of this work lies in correlating the experimental findings with actual PV operating conditions, providing valuable insights for the design and optimization of PHP-based passive cooling systems for photovoltaic applications.

EXPERIMENT

This section outlines the experimental methodology adopted to evaluate the thermal characteristics of the pulsating heat pipe. Details regarding the system design and testing procedure are presented in the subsequent subsection.

Pulsating Heat Pipe Design

This research used a single-turn closed-loop PHP model from a copper tube. Copper was chosen because of its high thermal conductivity. The working fluids selected in this study were methanol and ethanol, the thermophysical properties of which can be found in **Table 1**. There are some constraints in determining a PHP's internal pipe diameter (D). These constraints are defined by Bond number (Bo), a dimensionless number that measures the importance of gravitational forces compared to the surface tension force of a liquid surface. The Bond number can be calculated using Equation (1) **[20]**.

$$B_O = \sqrt{\frac{g(\rho_l - \rho_g)}{\sigma} {D_h}^2} \tag{1}$$

where D [m] is the inner diameter of the pipe; ρ_l [kg/m^3] is the density of the working fluid; ρ_g [kg/m^3] is the density of the vapor; σ is the surface tension [N/m]; and g is the gravitational acceleration [m/s^2].

Research conducted by Ahmad et al. **[35]** established a criterion stating that if Bo ≤ 2, the effect of the working fluid's surface tension will be greater than that of gravity. As a result, liquid plugs and vapor slugs will form inside the pipe. The following Equation (2) shows the upper and inner limits for a PHP internal diameter **[23]**:

$$0.7\sqrt{\frac{\sigma}{g(\rho_l - \rho_g)}} \leq D_h \leq 2\sqrt{\frac{\sigma}{g(\rho_l - \rho_g)}} \tag{2}$$

Table 1. Thermophysical properties of methanol and ethanol.

Working fluids	Boiling temperature (°C)	Dynamic viscosity (Pa.s)	Surface tension (N/m)	Density (kg/m^3)	Thermal conductivity (W/m.K)
Methanol	64.7	0.000547	0.02766	791	0.202
Ethanol	78.3	0.001074	0.02775	789	0.171

Based on the fluid's thermophysical properties and using Equation (2), the lower and upper limits for the internal diameter of a PHP system with ethanol and methanol working fluid were calculated at 1.15 mm and 3.3 mm, respectively. Based on the calculation result and the availability of the copper tube in the market, the selected copper tube outer and internal diameters were 4 mm and 2 mm, respectively.

The ratio between the evaporator and condenser section lengths was set at 0.8, which was within the optimum range and has been proven to result in low thermal resistance **[21]**. The ratio of the adiabatic section to the total length was set at 0.2 based on the works of Li et al. **[24]**. Therefore, the length of the evaporator, adiabatic, and condenser sections was 250 mm, 140 mm, and 312.5 mm, respectively. In addition, the heat pipes were seated onto a

semicircular, grooved plate to improve their contact area with the heating plate. The grooved plate was made of aluminum, chosen for its high thermal conductivity, to ensure efficient heat transfer from the heat source to the evaporator section. Furthermore, the adiabatic section was insulated using an ethylene propylene diene monomer (EPDM) rubber to prevent heat loss. The PHP system dimension and schematic can be found in **Figure 1**.

Experimental Setup

An electrical heating plate (20 x 15 cm) was used as the heat source. The plate's heating power was regulated using a 220 V, 500 W alternating current (AC) voltage regulator and monitored with a digital AC power meter with ±2 % accuracy. This setup ensured a stable heat input into the PHP. To minimize heat loss, the bottom of the heating plate was insulated with a double layer of rockwool. The heating plate was tilted at a 10° inclination angle to replicate a PV module installation. This inclination angle was kept the same throughout the experiments.

Ten Type-T thermocouples with a quoted accuracy of ± 0.5 °C were strategically placed on the outer wall of the PHP tube and heating plate. Three (T3 to T5), two (T6 and T7), and three (T8 to T10) thermocouples were placed at the evaporator, adiabatic, and condenser sections, respectively. The remaining two thermocouples (T1 and T2) were placed on the heating plate. All thermocouples were calibrated against an ASTM 9C thermometer with a range of 0-100 °C. A pressure transmitter, with a -1 to 1 bar range and a ± 1% accuracy , was used to monitor the system pressure. The analog signals from the thermocouples and pressure transmitter were sent to a 24-bit Labjack U6-Pro data acquisition module, supplemented with a CB-37 expansion board. A laptop was used for the real-time measurement display and data logging. The sampling period for data collection was set at 1-second intervals.

The charging system consists of a vacuum pump, a manifold, and a syringe. A syringe was used to charge the system with the working fluid to the predetermined filling ratio. A vacuum pump was then used to remove the non-condensable gases from the PHP. Once the internal pressure reached the required value, the valve manifold was then closed to stabilize the system for a period. During this process, the PHP system pressure was monitored to check for leakage. A constant pressure condition was established and verified prior to the commencement of the experiment to preclude any leaks**.** The overall experimental setup can be seen in **Figure 1**.

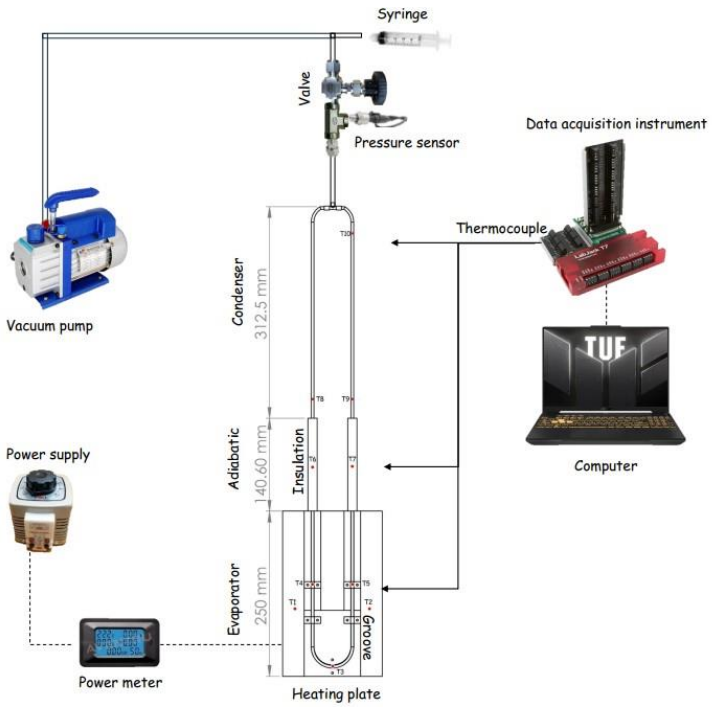

Figure 1. Experimental setup.

Experimental Procedure and Data Processing

A total of 72 experiments were conducted. Using a syringe, the PHP was filled with working fluid at a specified filling ratio. Then, the system's initial pressures were varied using the charging system and procedure mentioned in Sub-section 2.2. The thermal performance and startup characteristics of the system were then tested under several heat inputs. Once completed, the tests were repeated for the whole variation of initial pressure, filling ratio, and working fluid. The experimental parameters can be found in **Table 2**.

Table 2. Experimental parameters

Parameter	Value
Working fluid	Methanol, ethanol
Filling ratio	35%, 45%, 55%
Initial pressure (absolute)	30 kPa, 50 kPa, 100 kPa
Heat input	13.8 W, 29 W, 45 W, 60 W

The PHP's thermal resistance is calculated using the following Equation (3) **[34]**:

$$R = \frac{\bar{T}_e - \bar{T}_c}{Q} \tag{3}$$

where R [°C/W] is the thermal resistance, Q [W] is the heat input into the system, while $\bar{T}_e$ [°C] and $\bar{T}_c$ [°C] are the average evaporator and condenser sections' temperature, which are calculated using Equations (2) and (3), respectively.

$$\bar{T}_e = \frac{1}{3}\sum_{i=3}^{5} T_i \tag{4}$$

$$\bar{T}_c = \frac{1}{3}\sum_{i=8}^{10} T_i \tag{5}$$

The estimated temperature drops in the PV if the prototype is installed can be calculated using Equations (4), (5), and (6):

$$Q_{in} = m \times c_p \times \Delta T_{modul} \tag{6}$$

$$\frac{Q_{out}}{t} = h \times A \times \Delta T_{PHP} \tag{7}$$

$$T_{new} = \overline{T_{modul}} - \left(\Delta T_{modul} - \Delta T_{cooling}\right) \quad (8)$$

where Q_{in} [J] is the heat produced by solar panels, m [kg] is the mass of the solar module, c_p is the specific heat of the mixed material in solar panels with values 751 [J/kg.K] [36], ΔT_{modul} [°C] is the temperature difference between the final (after heated by the Sun) and initial temperature of the panel, while Q_{out} [W] is the heat dissipated by PHP, t [s] is the working time of PHP, h [W/m.K] is the free convection coefficient, A [m^2] is the area of the PHP condenser, ΔT_{PHP}[°C] is the temperature difference between the condenser and the surroundings, T_{new} [°C] is the module's temperature after cooling, $\overline{T_{modul}}$ [°C] is the average temperature of the solar panel in Bandung, Indonesia, which is set at 51.45 [°C] [33], and $\Delta T_{cooling}$ [°C] is the cooling temperature carried out by PHP.

The measurements' uncertainties were quantified by combining the systematic and random uncertainties using the following Equation (7) [37].

$$W_{\bar{x}} = (B_x^2 + P_x^2)^{1/2} \quad (9)$$

where $W_{\bar{x}}$ is the total uncertainty, B_x is the systematic uncertainty taken from the instruments' specified accuracy, and P_x is the random uncertainty computed from the measurement samples' standard error of the mean. In addition, the total uncertainty was evaluated using a confidence level of 95%. The calculated uncertainties for each measurement can be found in Table 3.

Table 3. Measurement uncertainties

Measurement	Total Uncertainties [%]
Evaporator average temperature, $\bar{T}_e$	± 1.1
Condenser average temperature, $\bar{T}_c$	± 1.2
Heat input, Q	± 2.0
Pressure, P	± 2.8
Filling Ratio, FR	± 2.2

RESULT AND DISCUSSION

Several variables were investigated to determine their effects on the startup and thermal performance of the pulsating heat pipe (PHP). These variables were the working fluid, filling ratio, initial pressure, and heat input.

A test without the working fluid was conducted to ensure that the observations afterward were solely due to the presence of the fluid. The plate was heated with a 45 W heating power, and the temperatures of the heat plate and empty-PHP sections were observed as shown in Figure 2. PHP temperature plot: empty pipe and at 45 W power input. However, there were no temperature fluctuations on the PHP's evaporator and condenser sections, which is a tell-tale of a functioning PHP. Indeed, the temperature increment observed in the PHP section was due to the conductivity of the copper tube itself. Clement and Wang [34] reported similar findings.

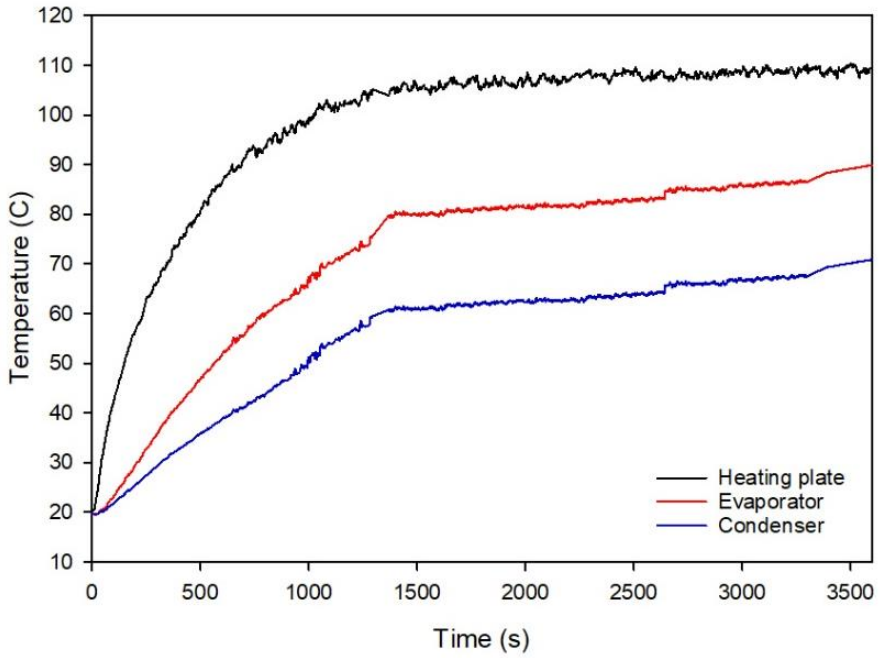

Figure 2. PHP temperature plot: empty pipe and at 45 W power input.

Effect of Initial Pressure

The initial pressure of a PHP system significantly affects the thermophysical properties of the working fluid, such as its boiling point. For example, at a pressure of 100 kPa, the boiling point of methanol is 64.7 °C, while at 50 kPa and 30 kPa pressure, the boiling point decreases to 47.3 °C and 36.5 °C, respectively. Similarly, the boiling point of ethanol, which is initially 78.4°C at 100 kPa, drops to 61.5 °C and 50.4 °C at 50 kPa and 30 kPa pressure, respectively.

Figure 3. Time to reach onset of pulsation for methanol with a FR 55%, 45 W power input and initial pressure of (a) 30 kPa, (b) 50 kPa, (c) 100 kPa, and (d) Start-up time comparison. shows the experimental results using methanol as the working fluid at different initial pressures, with the same filling ratio of 55% and the same heat input condition of 45 W. The result shows that the fastest initiation time of 264 s was achieved by an initial pressure of 30 kPa. At higher initial pressures, the startup time is slightly slower, as illustrated in **Figure 3**. Time to reach onset of pulsation for methanol with a FR 55%, 45 W power input and initial pressure of (a) 30 kPa, (b) 50 kPa, (c) 100 kPa, and (d) Start-up time comparison. and **Figure 3**. Time to reach onset of pulsation for methanol with a FR 55%, 45 W power input and initial pressure of (a) 30 kPa, (b) 50 kPa, (c) 100 kPa, and (d) Start-up time comparison.. An increase in initial pressure resulted in a longer startup time, with measured durations of 496 s and 1165 s corresponding to initial pressures of 50 kPa and 100 kPa, respectively. This phenomenon occurs due to the increased boiling temperature as the initial pressure increases. At an absolute pressure of 30 kPa, pulsation began at a lower evaporator temperature of 47 °C, whereas at 50 kPa and 100 kPa, the corresponding evaporator temperatures required for pulsation were 49 °C and 62 °C, respectively. **Figure 3**. Time to reach onset of pulsation for methanol with a FR 55%, 45 W power input and initial pressure of (a) 30 kPa, (b) 50 kPa, (c) 100 kPa, and (d) Start-up time comparison. illustrates the relationship between temperature and pressure at the initiation of pulsation. This relation gives confidence that pulsation has started. **Figure 3**. Time to reach onset of pulsation for methanol with a FR 55%, 45 W power input and initial pressure of (a) 30 kPa, (b) 50 kPa, (c) 100 kPa, and (d) Start-up time comparison. shows the relationship between heat transfer rate (power), initial pressure, and start-up time. Despite all the pressure, higher power reduced the start-up time. Nucleation and bubbling are accelerated when the power is increased.

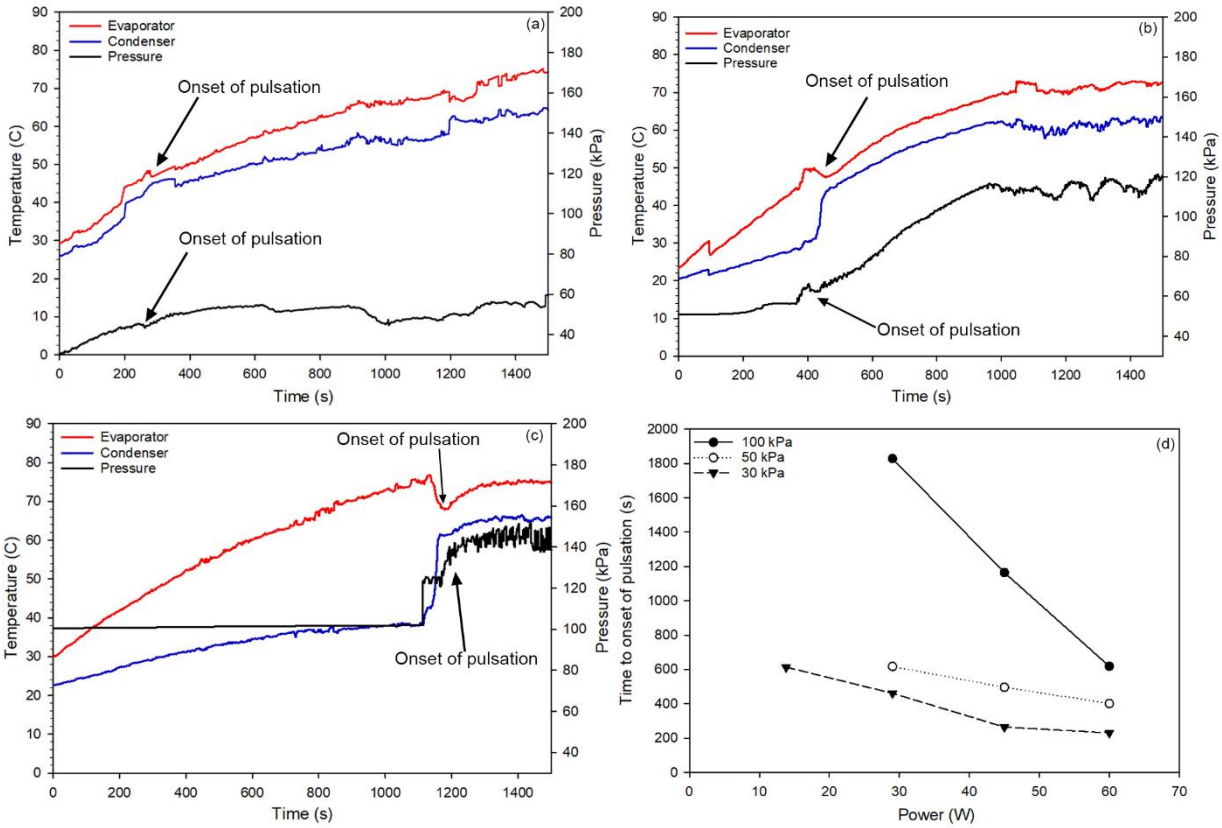

Figure 3. Time to reach onset of pulsation for methanol with a FR 55%, 45 W power input and initial pressure of (a) 30 kPa, (b) 50 kPa, (c) 100 kPa, and (d) Start-up time comparison.

The experimental results of using ethanol as the working fluid are shown in **Figure 4**. Time to reach onset of pulsation for ethanol with a FR 55%, 45 W power input and initial pressure of (a) 30 kPa, (b) 50 kPa, (c) 100 kPa, and (d) Start-up time comparison. A similar trend to the methanol working fluid was found in the ethanol working fluid. The time taken for the onset of pulsation at a pressure of 30 kPa became the fastest, with a time of 559 s, as seen in **Figure 4**. Time to reach onset of pulsation for ethanol with a FR 55%, 45 W power input and initial pressure of (a) 30 kPa, (b) 50 kPa, (c) 100 kPa, and (d) Start-up time comparison.. As the initial pressure increased, the onset of pulsation became longer, as seen from the test with an initial pressure of 50 kPa in **Figure 4**. Time to reach onset of pulsation for ethanol with a FR 55%, 45 W power input and initial pressure of (a) 30 kPa, (b) 50 kPa, (c) 100 kPa, and (d) Start-up time comparison. and 100 kPa in **Figure 4**. Time to reach onset of pulsation for ethanol with a FR 55%, 45 W power input and initial pressure of (a) 30 kPa, (b) 50 kPa, (c) 100 kPa, and (d) Start-up time comparison. , which are 999 s and 1173 s, respectively. Ethanol has a higher boiling temperature compared to methanol at the same pressure. That higher boiling temperature is responsible for the longer start-up time of ethanol compared to methanol. Comparison between the onset of pulsation time for different power inputs and initial pressure for a PHP using ethanol working fluid at a 55% filling ratio is presented in **Figure 4**. Time to reach onset of pulsation for ethanol with a FR 55%, 45 W power input and initial pressure of (a) 30 kPa, (b) 50 kPa, (c) 100 kPa, and (d) Start-up time comparison.. As shown in **Figure 4**. Time to reach onset of pulsation for ethanol with a FR 55%, 45 W power input and initial pressure of (a) 30 kPa, (b) 50 kPa, (c) 100 kPa, and (d) Start-up time comparison., reducing the initial pressure accelerated the onset of pulsation by lowering the boiling point. However, the startup time taken for the ethanol working fluid was longer when compared to the methanol working fluid under the same initial pressure, filling ratio, and heat input conditions.

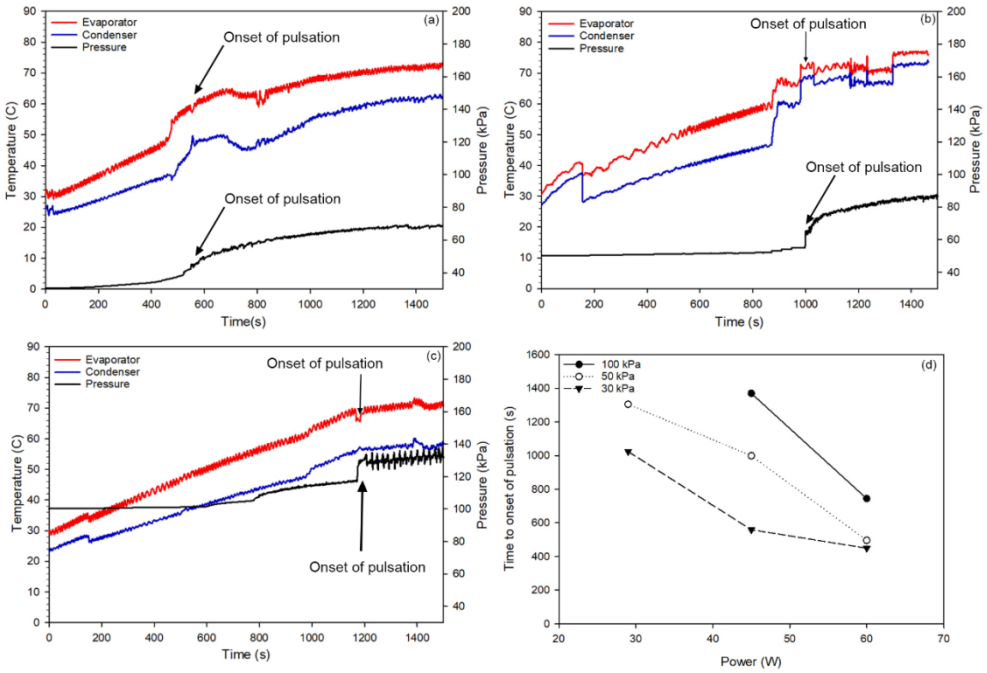

Figure 4. Time to reach onset of pulsation for ethanol with a FR 55%, 45 W power input and initial pressure of (a) 30 kPa, (b) 50 kPa, (c) 100 kPa, and (d) Start-up time comparison.

The experimental results shown in **Figure 5** indicate that the PHP operating at an initial pressure of 30 kPa exhibited the lowest temperature difference of 5.4 °C, compared with the tests conducted at 50 kPa and 100 kPa, which showed temperature differences of 7.3 °C and 8.5 °C, respectively. The fluctuations in the evaporator and condenser temperatures are shown in **Figure 5(a)**. Average evaporator and condenser temperature for methanol 30 kPa suggested a more stable operation compared with **Figure 5(b)** and **Figure 5(c)**. These fluctuations implied that the system was approaching a steady state, indicating that the working fluid performance at 30 kPa was more stable. Furthermore, the average evaporator temperature at 100 kPa was the highest (82.8 °C), while at 30 kPa, it was the lowest (80 °C).

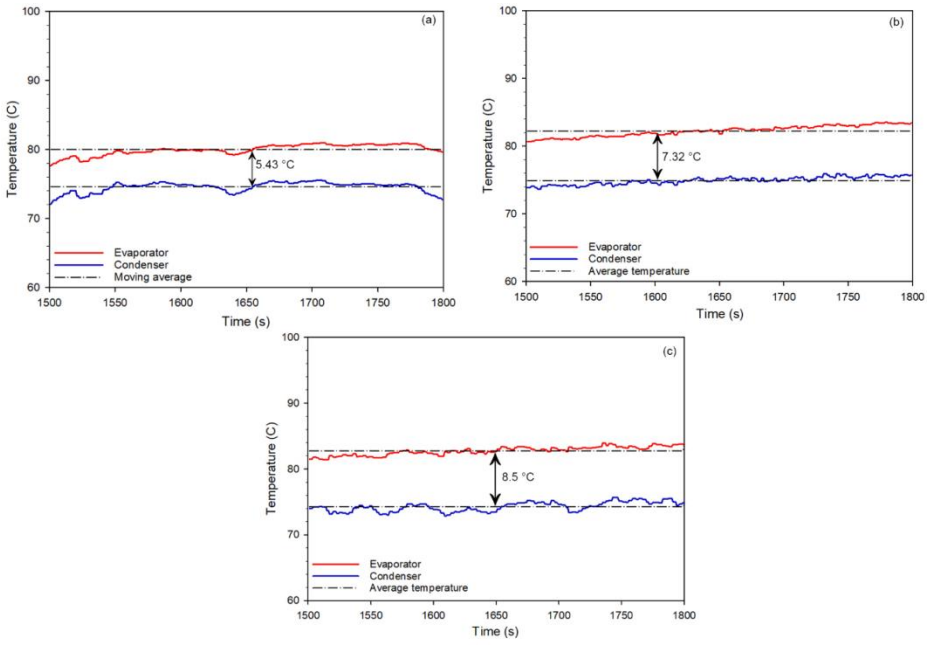

Figure 5. Average evaporator and condenser temperature for methanol with FR 55%, 60 W power input, and an initial pressure of (a) 30 kPa, (b) 50 kPa, (c) 100 kPa.

The results for the ethanol working fluid showed a similar trend, as illustrated in **Figure 6** Average evaporator and condenser temperature of ethanol FR 55% 60 W (a) 30 kPa, (b) 50 kPa, (c) 100 kPa.. The smallest temperature difference between the evaporator and condenser was observed at an initial pressure of 30 kPa, with a value of 7.3 °C, compared to 10.1 °C and 12.5 °C at 50 kPa and 100 kPa, respectively. This trend was consistent with the thermal performance measurements obtained for methanol. However, the temperature differences for ethanol were slightly higher, as ethanol requires more heat input to initiate and sustain pulsation. When excess heat is absorbed by ethanol, the temperature difference between the evaporator and the environment becomes larger than that of methanol, resulting in a higher thermal resistance for ethanol.

From these observations, it can be concluded that increasing the initial pressure leads to a higher temperature difference between the evaporator and condenser, thereby increasing the overall thermal resistance, as shown in **Figure 6** Average evaporator and condenser temperature of ethanol FR 55% 60 W (a) 30 kPa, (b) 50 kPa, (c) 100 kPa.. This effect became more pronounced at higher initial pressures.

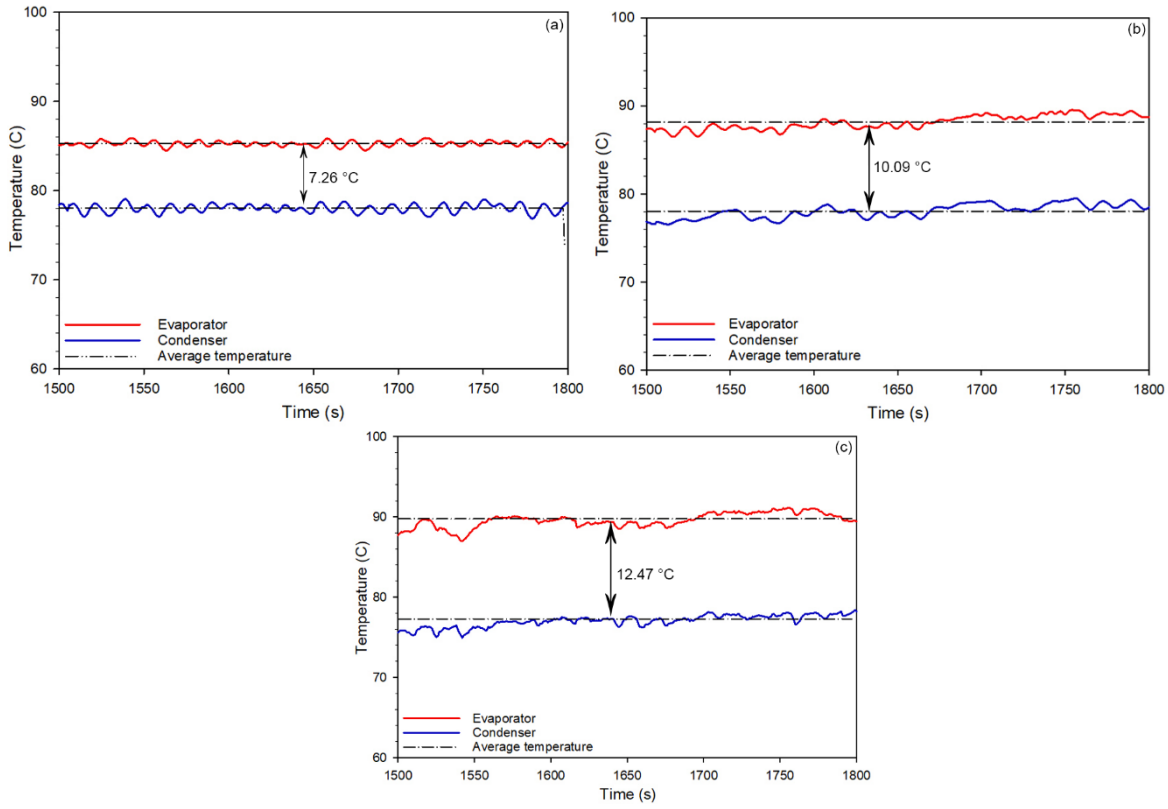

Figure 6 Average evaporator and condenser temperature of ethanol FR 55% 60 W (a) 30 kPa, (b) 50 kPa, (c) 100 kPa.

Effect of Filling Ratio

Determining the appropriate filling ratio is crucial, since a low filling ratio can lead to the PHP experiencing a dry-out. Conversely, when the filling ratio approaches 100%, a significant performance decline occurs due to insufficient space for vapor circulation. Experimental data reported by Clement and Wang **[34]** further showed that filling ratios between 35% and 55% of the total volume reach a steady state much faster than those outside this range.

The experimental result on the effect of filling ratio variation at an initial pressure of 30 kPa, using ethanol and methanol as working fluids, is presented in **Figure 7**. Time to reach the onset of pulsation for a PHP with an initial pressure of 30 kPa and several power inputs, with a working fluid of (a) methanol, and (b) ethanol. The results show that increasing the filling ratio

delayed the onset of pulsation. A low filling ratio needs lower energy to start pulsation. Therefore, a lower filling ratio causes a faster start-up time. PHP using methanol as working fluid with a filling ratio (FR) of 35%, an initial pressure of 30 kPa, and a heat input of 60 W has the fastest start-up time, achieving pulsation in just 171 s as shown in **Figure 8**. The fastest start-up time for a PHP with ethanol working fluid was 390 s, achieved by a system with an initial pressure of 30 kPa, a filling ratio (FR) of 35%, and a 60 W power input, as can be seen in **Figure 8**. At other filling ratios, the startup times were slightly longer. Experimental results obtained at various filling ratios with an initial pressure of 30 kPa and the same power input showed that a filling ratio of 55% resulted in the longest startup time. It can be concluded that the smaller the filling ratio, the faster the startup process. This behavior occurred due to the reduced volume of working fluid inside the PHP; a smaller liquid volume required less energy for vaporization. Moreover, the larger vapor space available at lower filling ratios facilitated easier fluid evaporation and the earlier initiation of pulsation.

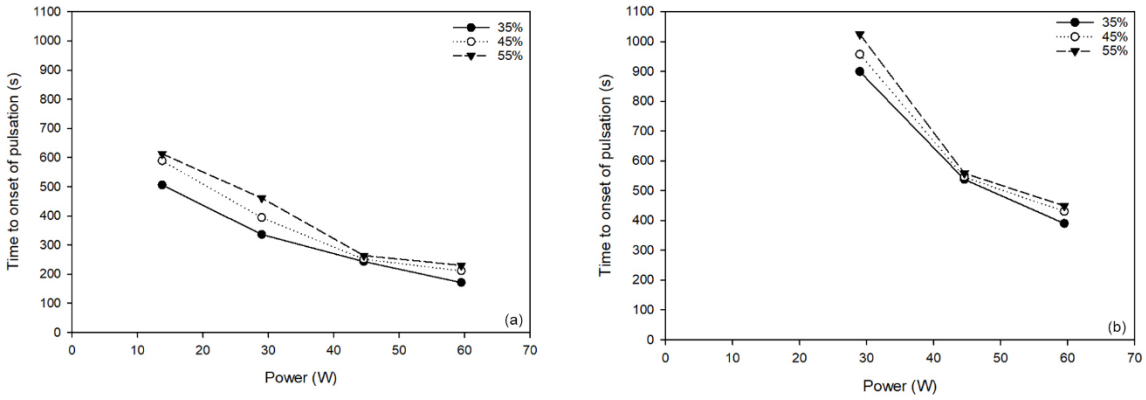

Figure 7. Time to reach the onset of pulsation for a PHP with an initial pressure of 30 kPa and several power inputs, with a working fluid of (a) methanol, and (b) ethanol.

The effect of filling ratio on the thermal performance was observed for ethanol and methanol working fluids with an initial pressure of 30 kPa. As seen in **Figure 8**, and **Figure 8** for both ethanol and methanol working fluids, the lowest thermal resistance was achieved with FR of 45%. **Figure 8**, and **Figure 8** also show that, for all filling ratios, the thermal resistance decreased as the power input increased. Higher power induces a faster startup time for pulsation. Faster pulsation directly contributes to better heat transfer from the evaporator to the condenser.

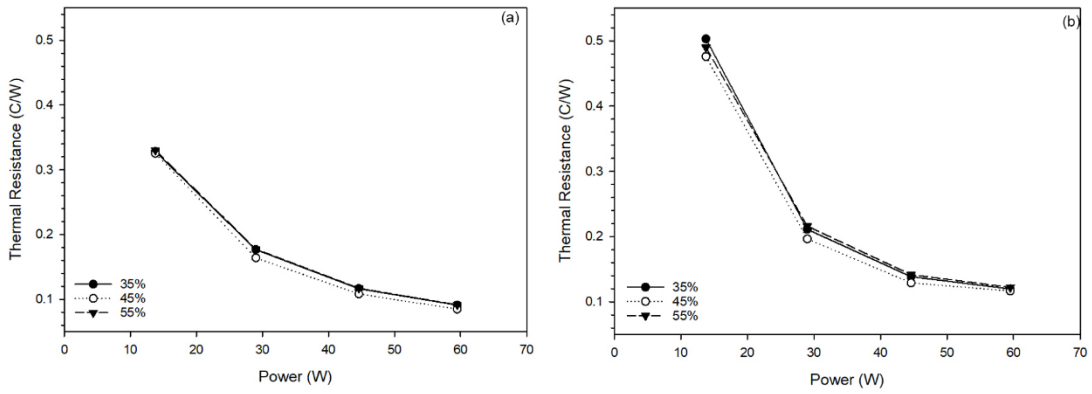

Figure 8. Thermal resistance comparison for a PHP with an initial pressure of 30 kPa at various power inputs, and a working fluid of (a) methanol, (b) ethanol.

The trend in thermal resistance for a PHP with methanol working fluid, at an initial pressure of 100 kPa, and varied FR and power input is illustrated in **Figure 9**. The higher power input increases evaporator temperature for all FR. At the FR of 35%, the average evaporator temperature was 47.4 °C, while at FR of 45% and 55%, the average evaporator temperature was slightly decreased to 47.3 °C and 47.0 °C, respectively. The difference between the evaporator and condenser temperatures influenced the thermal resistance value. Additionally, as the pressure increased, a greater amount of heat was required to start the pulsation. Consequently, at higher pressures, the working fluid exhibits a greater temperature difference, leading to higher thermal resistance compared to a working fluid at lower pressure.

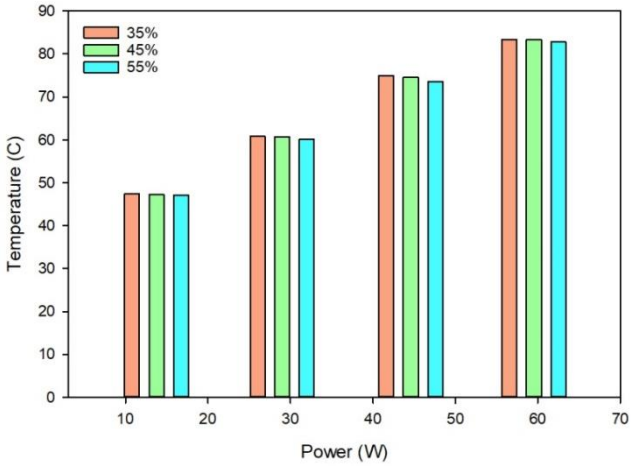

Figure **9**. Average evaporator temperature of a PHP system with methanol working fluids, at a 100 kPa initial pressure, and varied power inputs and FR.

Comparison with the Other Results

A comparison between the results of the present study and those reported in previous research was conducted. **Figure 10** presents a comparison between the current findings and those of Clement and Wang **[34]**. While the system used by Clement and Wang was a multi-loop PHP, the current study employed a single-loop configuration; however, both systems used methanol as the working fluid under an initial pressure of 100 kPa. In both studies, the filling ratio (FR) was varied to examine its effect on thermal resistance. As shown in **Figure 10** the results from both studies exhibited good agreement in trend, with the optimum thermal resistance occurring within an FR range of 40–45%. The slight differences in the thermal resistance values can be attributed to variations in the PHP configuration and experimental setup.

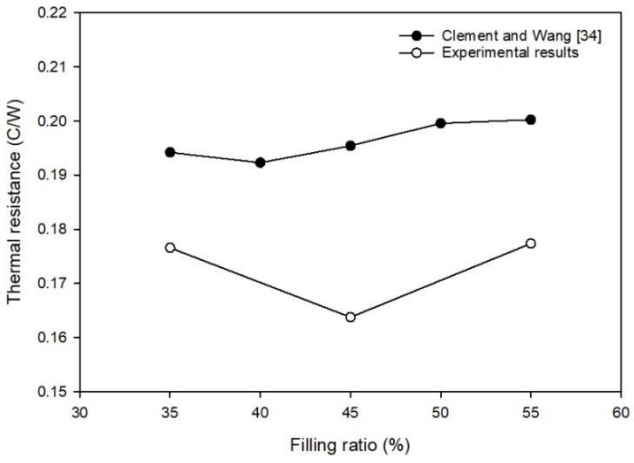

Figure 10. Comparison between the current study's results with Clement and Wang **[34]**.

Another comparison was made with the results reported by Qu et al. [29]. In their study, the initial pressure and filling ratio (FR) were kept constant while the power input was varied. They observed that as the power input increased, the thermal resistance decreased, although the rate of decrease gradually diminished. A similar trend was observed in the present study, as shown in **Figure 11**, the differences in thermal resistance values can be attributed to variations in the working fluid, water in Qu et al. [29], and methanol in the current study, as well as differences in operating conditions and experimental setup.

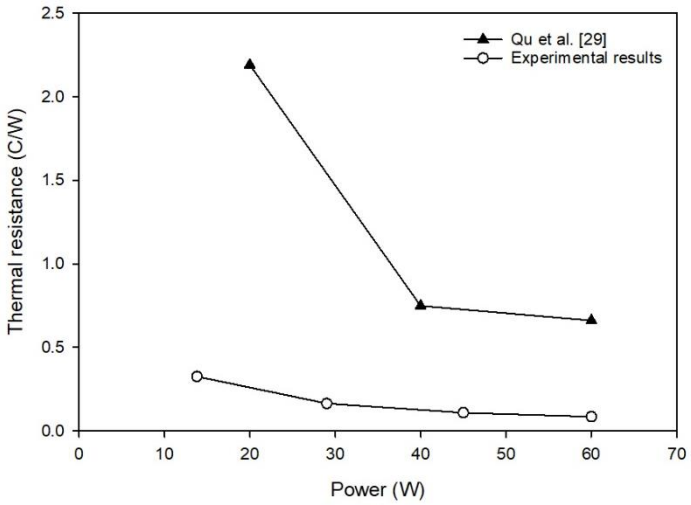

Figure 11. Comparison between the current study's results and those of Qu et al. [29].

Correlation to Field PV Conditions

The PHP system used in the experiment was a 1:3 scaled model of an actual system that will be used on a PV. In the experiment, the heating plate was used to emulate the heat generated by a PV. In actual condition, the PHP system will be attached to the back surface of a PV. The research conducted by Sutanto et al. [33] contain the information related to the temperature achieved by a PV placed at the same location in this study, namely Bandung, Indonesia. The PV temperature curve is presented in **Figure 12**.

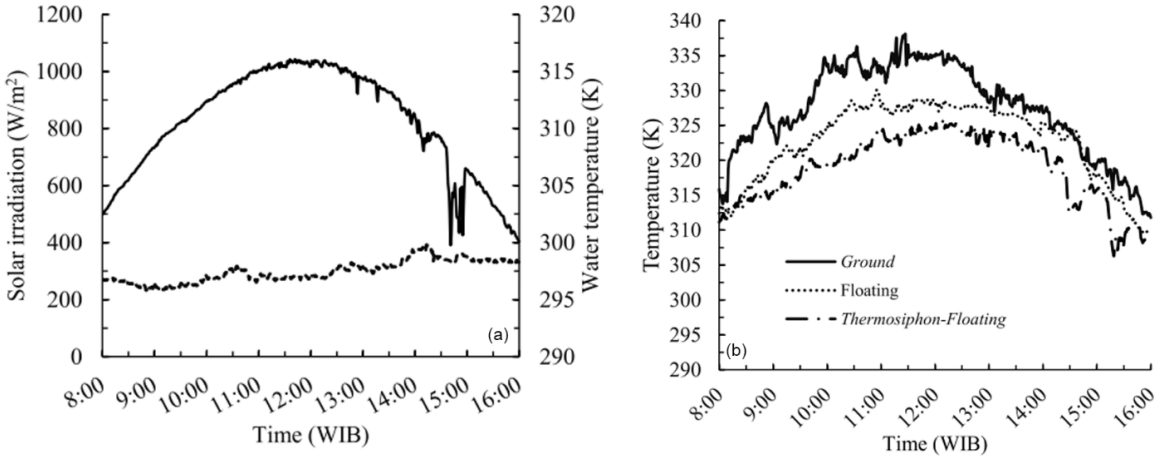

Figure 12. Operating condition of a PV installed in Bandung, Indonesia (a) solar irradiance, and (b) PV operating temperature [33].

In **Figure 12**, it can be observed that the PV temperature increased as the solar irradiance rose. The maximum temperature achieved by the PV at an irradiance of 1153 W/m² was 335.2 K, with an average operational temperature of 324.6 K. This average PV temperature is similar

to that achieved by the heating plate with a power input of 13.8 W. The temperature curve of the heating plate with a 13.8 W power input can be seen in **Figure 13**.

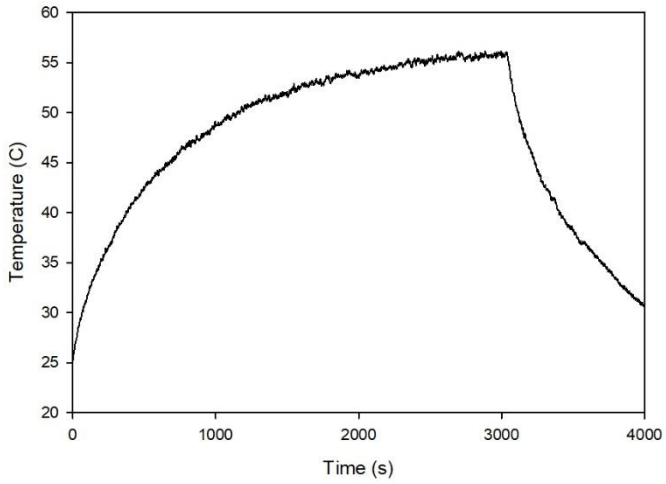

Figure 13. Heating plate temperature curve with a power input of 13.8 W.

The maximum temperature achieved by the heating plate with a 13.8 W power input, as shown in **Figure 13**, was 56.2 °C, equivalent to 329.15 K. This temperature range aligns with the PV temperatures reported in Sutanto et al. **[33]**. However, the integration of PHP with PV modules presents certain limitations. These include a geometric mismatch between the PHP tube and the flat PV surface, necessitating the use of an adhesive layer. Furthermore, the thermal performance is highly dependent on the working fluid's properties—such as its type, quantity, and mass—which govern the system's heat transport and dissipation capabilities. Although the energy density of solar irradiance differs from that of the heating plate, the findings of this study suggest that, for PHPs intended as passive cooling solutions, the working fluid should exhibit stable pulsation at a heat input of 13.8 W. Based on the experimental results, methanol at an initial pressure of 30 kPa is recommended as the most suitable working fluid. To achieve optimal thermal resistance, a filling ratio of 45% is suggested. The effective operation of methanol under these conditions is demonstrated in **Figure 14**.

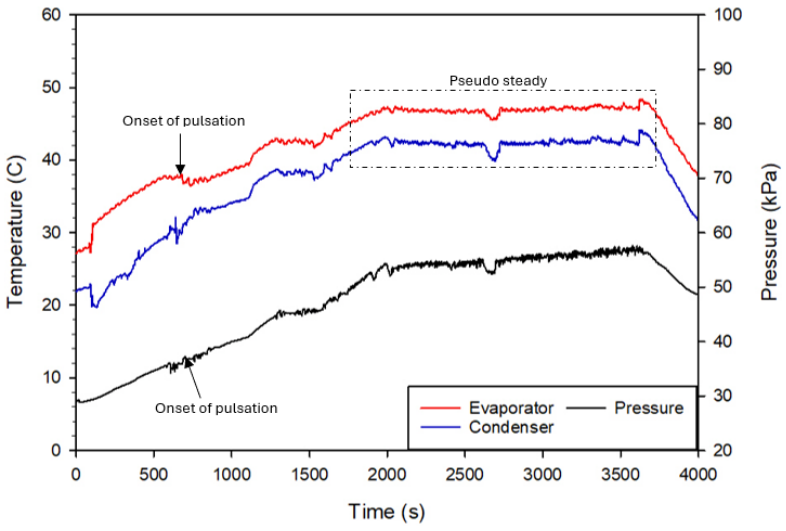

Figure 14. Full experimental results of PHP with methanol with an FR of 45%, and a 30 kPa initial pressure at 13.8 W power input.

Figure 14 demonstrates the effective performance of the PHP, as evidenced by the pressure fluctuations that closely follow the temperature trend, indicating sustained oscillatory motion

inside the PHP. The pseudo–steady state was reached faster at an initial pressure of 30 kPa compared to 50 kPa and 100 kPa. Although the startup time at 30 kPa was not the shortest, this configuration yields a significantly lower thermal resistance of 0.325 °C/W, compared to 0.485 °C/W and 0.606 °C/W at 50 kPa and 100 kPa, respectively. This improvement is attributed to the smaller average temperature difference between the evaporator and condenser at 30 kPa.

Furthermore, a filling ratio of 45% resulted in the lowest thermal resistance (0.325 °C/W), outperforming 35% (0.328 °C/W) and 55% (0.330 °C/W). Based on these findings, installing six PHP units on the rear side of a photovoltaic (PV) panel can be expected to reduce the panel temperature according to Equations (4), (5), and (6). The calculation yields a new panel temperature of 46.4 °C, corresponding to a temperature reduction of approximately 5.1 °C. This result confirms that the addition of PHP-based passive cooling can effectively enhance the thermal management of solar panels.

CONCLUSIONS

The pulsating heat pipe (PHP) is designed to provide passive cooling capabilities, and the investigated parameters are matched under conditions representative of actual PV module operation. The results show that methanol is the most suitable working fluid, offering the fastest startup and the lowest thermal resistance due to its favorable thermophysical properties. Among the tested filling ratios, 35% provides the quickest startup because of the smaller liquid volume and larger vapor space that facilitates pulsation, whereas 45% yields the lowest thermal resistance. Increasing the initial pressure raises the evaporator temperature and the temperature difference between the evaporator and condenser, thereby increasing the thermal resistance. The optimal performance is achieved at an initial pressure of 30 kPa, where the thermal resistance reaches its minimum. Moreover, increasing the input power accelerates startup and reduces thermal resistance. The highest evaporator temperature occurs at a 35% filling ratio, compared to 45% and 55%. Overall, the combination of methanol as the working fluid, a 45% filling, an initial pressure of 30 kPa, and an input power of 13.8 W shows compatibility with typical PV module operating temperatures, making it the recommended configuration for passive PV cooling. Under these conditions, integrating PHPs on the rear side of the solar panel can potentially reduce the panel temperature by up to 5.1 °C, confirming the system's effectiveness for passive thermal management.

ACKNOWLEDGEMENT(S)

Financial support for this work was provided by the Faculty of Mechanical and Aerospace Engineering (FMAE) ITB through the 2023–2024 P2MI grant scheme. Additional support was received from the Research Center for New and Renewable Energy ITB, which enabled the completion of this study.

NOMENCLATURE

Bo	bond number	
g	gravity	[m/s^2]
R	thermal resistance	[°C/W]
$\overline{T_e}$	average evaporator temperature	[°C]
$\overline{T_c}$	average condenser temperature	[°C]
T_i	initial temperature	[°C]
Q	heat produced by solar panels	[W]
Q_{in}	heat input to the system	[W]
m	mass of solar module	[kg]
Q_{out}	heat dissipated by PHP	[W]
C_p	specific heat of mixed material in solar panels	[kJ/kg.K]

ΔT_{modul}	difference in temperature between the panel and the environment	[°C]
t	working time of PHP	[s]
h	free convection coefficient	[W/m^2.K]
A	area of the condenser section in PHP	[m^2]
ΔT_{PHP}	temperature difference between the evaporator and the surround	[°C]
T_{new}	module temperature after cooling	[°C]
T_{modul}	average temperature of solar panel in Bandung	[°C]
$T_{cooling}$	cooling temperature carried out by PHP	[°C]

Greek letters

ρ_l	density of liquid phase	[kg/m^3]
ρ_g	density of gas phase	[kg/m^3]
σ	surface tension	[N/m]

Abbreviations

PHP	Pulsating Heat Pipe
OHP	Oscillating Heat Pipe
GHG	Greenhouse Gas

REFERENCES

1. Z. T. Mirza, T. Anderson, J. Seadon, and A. Brent, "A thematic analysis of the factors that influence the development of a renewable energy policy," *Renew. Energy Focus* , vol. 49, no. February, p. 100562, 2024, https://doi.org/10.1016/j.ref.2024.100562.
2. C. Le Quéré *et al.*, "Temporary reduction in daily global CO2 emissions during the COVID-19 forced confinement," *Nat. Clim. Chang.*, vol. 10, no. 7, pp. 647–653, 2020, https://doi.org/10.1038/s41558-020-0797-x.
3. H. Alizadeh, M. Alhuyi Nazari, R. Ghasempour, M. B. Shafii, and A. Akbarzadeh, "Numerical analysis of photovoltaic solar panel cooling by a flat plate closed-loop pulsating heat pipe," *Sol. Energy*, vol. 206, no. May 2019, pp. 455–463, 2020, https://doi.org/10.1016/j.solener.2020.05.058.
4. M. Aramesh, F. Pourfayaz, and A. Kasaeian, "Numerical investigation of the nanofluid effects on the heat extraction process of solar ponds in the transient step," *Sol. Energy*, vol. 157, no. August, pp. 869–879, 2017, https://doi.org/10.1016/j.solener.2017.09.011.
5. E. Skoplaki and J. A. Palyvos, "On the temperature dependence of photovoltaic module electrical performance: A review of efficiency/power correlations," *Sol. Energy*, vol. 83, no. 5, pp. 614–624, 2009, https://doi.org/10.1016/j.solener.2008.10.008.
6. P. Dwivedi, K. Sudhakar, A. Soni, E. Solomin, and I. Kirpichnikova, "Advanced cooling techniques of P.V. modules: A state of art," *Case Stud. Therm. Eng.*, vol. 21, no. December 2019, p. 100674, 2020, https://doi.org/10.1016/j.csite.2020.100674.
7. B. Sutanto *et al.*, "Design and analysis of passively cooled floating photovoltaic systems," *Appl. Therm. Eng.*, vol. 236, no. PD, p. 121801, 2024, https://doi.org/10.1016/j.applthermaleng.2023.121801.
8. A. S. Barrak, A. A. M. Saleh, and Z. H. Naji, "Energy Saving of Air Conditioning System by Oscillating Heat Pipe Heat Recovery Using Binary Fluid," *4th Sci. Int. Conf. Najaf, SICN 2019*, pp. 178–183, 2019, https://doi.org/10.1109/SICN47020.2019.9019354.
9. Y. Chen, Y. He, and X. Zhu, "Flower-type pulsating heat pipe for a solar collector," *Int. J. Energy Res.*, vol. 44, no. 9, pp. 7734–7745, 2020, https://doi.org/10.1002/er.5505.

10. Y. F. Maydanik, V. I. Dmitrin, and V. G. Pastukhov, "Compact cooler for electronics on the basis of a pulsating heat pipe," *Appl. Therm. Eng.*, vol. 29, no. 17–18, pp. 3511–3517, 2009, https://doi.org/10.1016/j.applthermaleng.2009.06.005.
11. C. Min, X. Gao, F. Li, and K. Wang, "Thermal performance analyses of pulsating heat pipe for application in proton exchange member fuel cell," *Energy Convers. Manag.*, vol. 259, no. November 2021, p. 115566, 2022, https://doi.org/10.1016/j.enconman.2022.115566.
12. M. E. B. M. Roslan and I. Hassim, "Solar PV system with pulsating heat pipe cooling," *Indones. J. Electr. Eng. Comput. Sci.*, vol. 14, no. 1, pp. 311–318, 2019, https://doi.org/10.11591/ijeecs.v14.i1.pp311-318.
13. S. B. Paudel and G. J. Michna, "Effect of inclination angle on pulsating heat pipe performance," *ASME 2014 12th Int. Conf. Nanochannels, Microchannels, Minichannels, ICNMM 2014, Collocated with ASME 2014 4th Jt. US-European Fluids Eng. Div. Summer Meet.*, pp. 1–6, 2014, https://doi.org/10.1115/ICNMM2014-22016.
14. Q. Cai, C. L. Chen, and J. F. Asfia, "An investigation of temperature characteristics of pulsating heat pipe," *Am. Soc. Mech. Eng. Heat Transf. Div. HTD*, vol. 376 HTD, no. 1, pp. 7–12, 2005, https://doi.org/10.1115/IMECE2005-79597.
15. Z. Du and X. Lin, "Research Progress on Experimental Optimization for Heat Performance of Pulsating Heat Pipe," *IOP Conf. Ser. Earth Environ. Sci.*, vol. 512, no. 1, 2020, https://doi.org/10.1088/1755-1315/512/1/012007.
16. M. Groll and S. Khandekar, "State of the art on pulsating heat pipes," *Proc. Second Int. Conf. Microchannels Minichannels*, pp. 33–44, 2004, https://doi.org/10.1115/icmm2004-2318.
17. H. Alizadeh, R. Ghasempour, M. B. Shafii, M. H. Ahmadi, W. M. Yan, and M. A. Nazari, "Numerical simulation of PV cooling by using single turn pulsating heat pipe," *Int. J. Heat Mass Transf.*, vol. 127, pp. 203–208, 2018, https://doi.org/10.1016/j.ijheatmasstransfer.2018.06.108.
18. J. Kim and S. J. Kim, "Experimental investigation on working fluid selection in a micro pulsating heat pipe," *Energy Convers. Manag.*, vol. 205, no. December 2019, p. 112462, 2020, https://doi.org/10.1016/j.enconman.2019.112462.
19. Z. Li *et al.*, "Operation analysis, response and performance evaluation of a pulsating heat pipe for low temperature heat recovery," *Energy Convers. Manag.*, vol. 222, no. March, p. 113230, 2020, https://doi.org/10.1016/j.enconman.2020.113230.
20. H. Ma, *Oscillating heat pipes*. 2015. https://doi.org/10.4271/2000-01-2375.
21. W. Shi, M. Li, H. Chen, and L. Pan, "Effect of evaporating-condensing length ratio and heat flux on starting and operating characteristic of pulsating heat pipe," *Appl. Therm. Eng.*, vol. 246, no. October 2023, p. 122963, 2024, https://doi.org/10.1016/j.applthermaleng.2024.122963.
22. S. Okazaki, H. Fuke, and H. Ogawa, "Performance of circular Oscillating Heat Pipe for highly adaptable heat transfer layout," *Appl. Therm. Eng.*, vol. 198, no. August, p. 117497, 2021, https://doi.org/10.1016/j.applthermaleng.2021.117497.
23. X. Han, X. Wang, H. Zheng, X. Xu, and G. Chen, "Review of the development of pulsating heat pipe for heat dissipation," *Renew. Sustain. Energy Rev.*, vol. 59, pp. 692–709, 2016, https://doi.org/10.1016/j.rser.2015.12.350.
24. M. Li, L. Li, and D. Xu, "Effect of number of turns and configurations on the heat transfer performance of helium cryogenic pulsating heat pipe," *Cryogenics (Guildf).*, vol. 96, no. April, pp. 159–165, 2018, https://doi.org/10.1016/j.cryogenics.2018.09.005.
25. A. Mucci, F. K. Kholi, J. Chetwynd-Chatwin, M. Y. Ha, and J. K. Min, "Numerical investigation of flow instability and heat transfer characteristics inside pulsating heat pipes with different numbers of turns," *Int. J. Heat Mass Transf.*, vol. 169, p. 120934, 2021, https://doi.org/10.1016/j.ijheatmasstransfer.2021.120934.

26. P. Charoensawan, S. Khandekar, M. Groll, and P. Terdtoon, "Closed loop pulsating heat pipes - Part A: Parametric experimental investigations," *Appl. Therm. Eng.*, vol. 23, no. 16, pp. 2009–2020, 2003, https://doi.org/10.1016/S1359-4311(03)00159-5.
27. X. Liu *et al.*, "Effect of evaporation and condensation section length ratio on thermal performance of aluminum flat plate heat pipe with different micro grooved wicks," *Appl. Therm. Eng.*, vol. 233, no. June, p. 121115, 2023, https://doi.org/10.1016/j.applthermaleng.2023.121115.
28. P. Charoensawan and P. Terdtoon, "Thermal performance of horizontal closed-loop oscillating heat pipes," *Appl. Therm. Eng.*, vol. 28, no. 5–6, pp. 460–466, 2008, https://doi.org/10.1016/j.applthermaleng.2007.05.007.
29. J. Qu, A. Zuo, F. Liu, and Z. Rao, "Quantitative analysis of thermal performance and flow characteristics of oscillating heat pipes with different initial pressure," *Appl. Therm. Eng.*, vol. 181, no. April, p. 115962, 2020, https://doi.org/10.1016/j.applthermaleng.2020.115962.
30. T. Hao, H. Ma, and X. Ma, "Heat transfer performance of polytetrafluoroethylene oscillating heat pipe with water, ethanol, and acetone as working fluids," *Int. J. Heat Mass Transf.*, vol. 131, pp. 109–120, 2019, https://doi.org/10.1016/j.ijheatmasstransfer.2018.08.133.
31. X. M. Zhang, J. L. Xu, and Z. Q. Zhou, "Experimental study of a pulsating heat pipe using fc-72, ethanol, and water as working fluids," *Exp. Heat Transf.*, vol. 17, no. 1, pp. 47–67, 2004, https://doi.org/10.1080/08916150490246546.
32. J. D. Bernardin and I. Mudawar, "A cavity activation and bubble growth model of the Leidenfrost point," *J. Heat Transfer*, vol. 124, no. 5, pp. 864–874, 2002, https://doi.org/10.1115/1.1470487.
33. B. Sutanto, Y. S. Indartono, A. T. Wijayanta, and H. Iacovides, "Enhancing the performance of floating photovoltaic system by using thermosiphon cooling method: Numerical and experimental analyses," *Int. J. Therm. Sci.*, vol. 180, no. May, p. 107727, 2022, https://doi.org/10.1016/j.ijthermalsci.2022.107727.
34. J. Clement and X. Wang, "Experimental investigation of pulsating heat pipe performance with regard to fuel cell cooling application," *Appl. Therm. Eng.*, vol. 50, no. 1, pp. 268–274, 2013, https://doi.org/10.1016/j.applthermaleng.2012.06.017.
35. H. Ahmad and S. Y. Jung, "Effect of active and passive cooling on the thermo-hydrodynamic behaviors of the closed-loop pulsating heat pipes," *Int. J. Heat Mass Transf.*, vol. 156, p. 119814, 2020, https://doi.org/10.1016/j.ijheatmasstransfer.2020.119814.
36. G. Notton, C. Cristofari, M. Mattei, and P. Poggi, "Modelling of a double-glass photovoltaic module using finite differences," *Appl. Therm. Eng.*, vol. 25, no. 17–18, pp. 2854–2877, 2005, https://doi.org/10.1016/j.applthermaleng.2005.02.008.
37. A. R. G. Anthony J. Wheeler, *Introduction to Engineering Experimentation*. 2004.

Paper submitted: 19.08.2025
Paper revised: 12.12.2025
Paper accepted: 21.12.2025